Journal of Quantitative Spectroscopy & Radiative Transfer 147 (2014) 196–206

Contents lists available at ScienceDirect

Journal of Quantitative Spectroscopy & Radiative Transfer

journal homepage: www.elsevier.com/locate/jqsrt

Effects of atmospheric water on the optical properties of soot aerosols with different mixing states

Tianhai Cheng*, Xingfa Gu, Yu Wu, Hao Chen

State Key Laboratory of Remote Sensing Science, Institute of Remote Sensing and Digital Earth, Chinese Academy of Sciences, Beijing 100101, China

ARTICLE INFO

Article history:
Received 24 March 2014
Received in revised form
15 May 2014
Accepted 2 June 2014
Available online 12 June 2014

Keywords:
Soot aerosol
Hygroscopic properties
Absorbing properties
Scattering properties
Climate change

ABSTRACT

Soot aerosols have become the second most important contributor to global warming after carbon dioxide in terms of direct forcing, which is the dominant absorber of visible solar radiation. The optical properties of soot aerosols depend strongly on the mixing mechanism of black carbon with other aerosol components and its hygroscopic properties. In this study, the effects of atmospheric water on the optical properties of soot aerosols have been investigated using a superposition T-matrix method that accounts for the mixing mechanism of soot aerosols with atmospheric water. The dramatic changes in the optical properties of soot aerosols were attributed to its different mixing states with atmospheric water (externally mixed, semi-embedded mixed, and internally mixed). Increased absorption is accompanied by a larger increase in scattering, which is reflected by the increased single scattering albedo. The asymmetry parameter also increased when increasing the atmospheric water content. Moreover, atmospheric water intensified the radiative absorption enhancement attributed to the mixing states of the soot aerosols, with values ranging from 1.5 to 2.5 on average at 0.870 μm. The increased absorption and scattering ability of soot aerosols, which is attributed to atmospheric water, exerted an opposing effect on climate change. These findings should improve our understanding of the effects of atmospheric water on the optical properties of soot aerosols and their effects on climate. The mixing mechanism for soot aerosols and atmospheric water is important when evaluating the climate effects of soot aerosols, which should be explicitly considered in radiative forcing models.

1. Introduction

Soot aerosols affect the energy budget of the Earth by absorbing solar radiation, influence cloud processes, and alter the melting of snow and ice cover [17,19,47]. Because the black carbon (BC) in soot aerosols dominates the absorption of visible solar radiation, soot aerosols are the second most important contributor of global warming after carbon dioxide in terms of direct forcing in the present-day atmosphere [21].

However, the uncertainties surrounding the net climate forcing from soot aerosols are substantial because little is known regarding the optical properties of soot aerosols. Comparing field and remote sensing observations with many climate models simulation indicates that the atmospheric absorption attributable to soot aerosols is too low in many climate models studies; these differences have not been extensively examined, nor are they well-understood [5].

The BC particles in soot aerosols are co-emitted with numerous other aerosols and aerosol precursor gases. Soon

* Corresponding author. Tel.: +86 10 64889562.
E-mail address: chength@radi.ac.cn (T. Cheng).

http://dx.doi.org/10.1016/j.jqsrt.2014.06.002
0022-4073/

after emission, the BC particles mix with other aerosol components in the atmosphere [49,37,13]. The optical properties of soot aerosols depend strongly on the mixing mechanism of BC with other aerosol components ([48,6,30]), as well as its hygroscopic properties [53,56,55,28]. Based on modeling and laboratory studies, the strong absorption abilities of soot mixed with other aerosols enhance the radiative forcing of the aerosol by up to three times compared to the externally mixed scenarios [21,14]. However, based on in-situ measurements on urban plumes, the aerosol absorption enhancement for mixed soot may have been overestimated in models [8,22,9].

Determining and explaining the BC mixing state with other aerosol species is highly complex and remains unresolved to date. The optical properties of soot aerosols can depend strongly on the morphology [26,25,24,23, 33,39,38]. The hygroscopicity of soot aerosols critically influences their optical properties [40,16,10]. How many ever climate models, the mixing mechanism of BC with other aerosol components and the water vapor in the ambient atmospheric remain largely unknown because the water and other semi-volatile species on the soot aerosol surface evaporate easily during the in-situ measurements performed under high-vacuum [51].

Due to the lack of reliable information on atmospheric water effects on soot aerosols optical properties and the critical importance of aerosols during radiative forcing assessments, this study aims to investigate the effects of atmospheric water on the optical properties of soot aerosols while determining the mixing mechanism for soot aerosols and atmospheric water. Theoretical simulations are required to quantify the mixing mechanism based on the volatile properties of water. The Multiple Sphere T-Matrix [35] was used to reconstruct the absorption properties and scattering properties of soot aerosols with different mixing states, extending the formulation to arbitrary configurations of spherical surfaces.

The enhancement in absorption due to the mixing states has been discussed in several previous theoretical studies ([21,14]) and has been observed in both laboratory and field experiments [8,28]. In this study, the effects of atmospheric water on the optical properties (absorption coefficient, single scattering albedo (SSA), and asymmetry parameter (ASY)) of soot aerosols with different mixing states (externally mixed, semi-embedded mixed, and internally mixed) have been investigated using theoretical studies. These findings should improve our understanding of the effects of atmospheric water on the optical properties of soot aerosols and their effects on the climate.

2. Mixing states of soot aerosols with atmospheric water

The in-situ and laboratory measurements [49,1,13] indicate that the pure BC particles consist of small spherical primary particles combined into branched and often-hydrophobic aggregates. Pure BC particles tend to be coated with a thin layer of other aerosol components in the atmosphere through the coagulation and condensation of secondary aerosol compounds. With the aging of the light absorbing carbon particles, most BC particles are thickly coated and tend to be compact. Coating BC particles with water-soluble compounds changes their hygroscopic properties [41,44,45, 55,27], which tend to be hydrophilic. For thinly coated light absorbing carbon aerosols, the BC particles are thinly coated by other aerosol components, and the morphology of the BC particles is still visible. For heavily coated light absorbing carbon aerosols, however, the BC particles are embedded into other aerosol components, and the morphology of BC particles is not visible.

To quantify the effects of water on the optical properties of soot aerosols in different mixing states, we assume that only three chemical compounds exist in the soot aerosols: black carbon (BC), sulfates, and water. Based on transmission electron microscopy (TEM) measurements [20,46,31,29,2] and the hygroscopicity of soot aerosols, the three mixing states of soot aerosols with and without water were modeled: externally mixed; semi-embedded mixed and internally mixed.

Fig. 1 shows a schematic image of the three mixing states. Fig. 1a shows the external mixture of pure BC and sulfate particles without water. Due to the hydrophilic properties of sulfate, in the wet condition, the sulfate tends to be coated with a water shell; the external mixture with water is shown in Fig. 1d. As the pure BC particles age, the aggregates can become semi-embedded (Fig. 1b) or internally mixed with the sulfate particles (Fig. 1c), and the corresponding hydrous mixing states are shown in Fig. 1e and f, which feature uniform water coatings.

The morphologies of the soot aerosols can be modeled using the parallel diffusion limited aggregation (DLA) algorithm [34]. The construction and morphology of the fractal clusters can be described by a well-known statistical scaling law:

$$N_s = k_0 \left(\frac{R_g}{a}\right)^{D_f} \tag{1}$$

$$R_g^2 = \frac{1}{N_s} \sum_{i=1}^{N_s} r_i^2 \tag{2}$$

where N_s is the number of monomers in the cluster, a is the mean radius of the monomer. k_0 is the fractal prefactor, D_f is the fractal dimension, R_g is the radius of gyration, which represents the deviation of the overall aggregate radius in a cluster, and r_i is the distance from the ith monomer to the center of the cluster.

For the sake of simplicity, the sulfate particles are treated as homogeneous spheres that are either coated or embedded within water. Water is treated as a uniform coating on the surface of sulfate particles. The radius of the sulfate particles (R_{su}) is used to reconstruct the sulfate particle, while the equivalent volume radius of water (R_w) is used to indicate the water content on the sulfate particles. For theoretical calculations, R_w is a multiple of the radius of the soot monomer (a). We chose three representatives R_w: $0a$ (0 μm), $12a$ (0.18 μm), $24a$ (0.36 μm).

To simulate these types of soot-containing mixtures, the surfaces of the soot-containing models do not overlap for the single scattering calculations, due to the limitations of the superposition T-matrix approach [36]. The external sulfate/water and soot aggregate mixtures can be modeled easily using a common DLA method. Moreover, the internal mixtures are modeled further based on the spherical constraints of the larger sulfate/water particle. The geometric center of

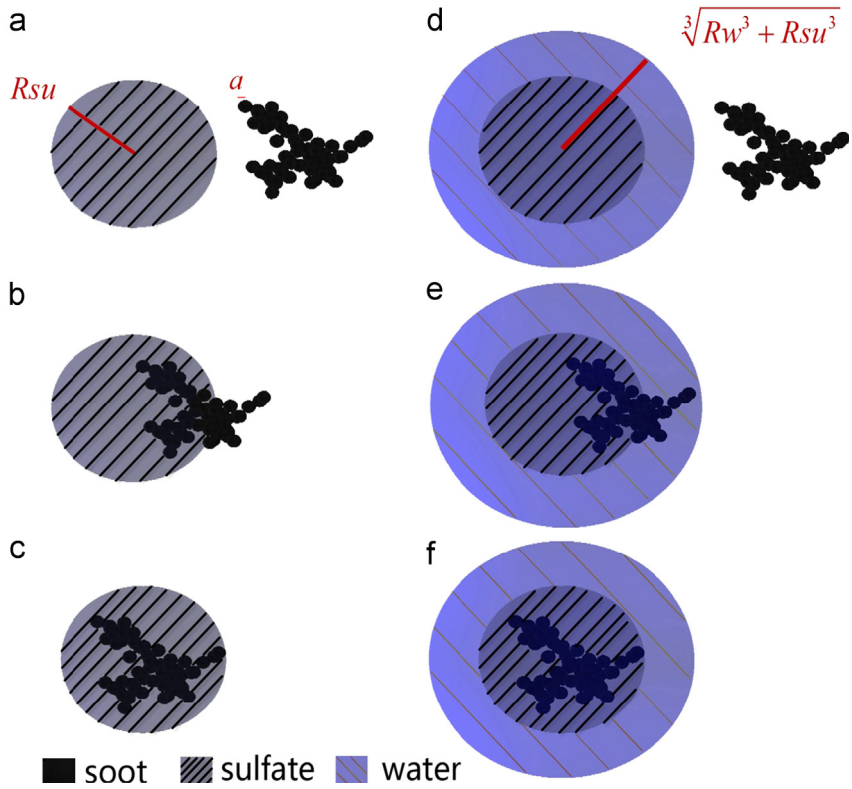

Fig. 1. Schematic images of the three mixing states of soot aerosols with or without water: (a) and (d) are the external mixing state of BC with sulfate particles, (b) and (e) are the semi-embedded mixing state of BC with sulfate particles, where BC is not uniformly coated by the sulfate particles, and (c) and (f) are the internally mixing state of BC with sulfate particle, where BC is heavily coated by sulfate particles. The black regions denote BC. The gray and blue regions denote sulfate and water, respectively. The radius of the sulfate particles (R_{su}) is used to reconstruct the sulfate particle, while the equivalent volume radius of water (R_w) is used to indicate the water content on the sulfate particles. a is the radius of the soot monomer. The surfaces of the soot-containing models do not overlap for calculations, due to the limitations of the superposition T-matrix approach. (For interpretation of the references to color in this figure legend, the reader is referred to the web version of this article.)

the internal mixtures is random, but the initial soot monomer and the sulfate are concentric. However, the semi-embedded models are divided into inner and outer clusters by the boundary of the larger sulfate/water sphere. First, pairs of monomers containing one or two inner monomers and an equal number of outer monomers make physical contact with each other as initial seeds (solid small spheres). Afterwards, the inner monomers and outer monomers of soot clusters aggregate (dashed small spheres). The aggregation process is constrained by the fractal parameters required for the morphology, including the fractal prefactor (k_0), fractal dimension (D_f) and the inner ($N_{s,in}$) and outer monomer numbers ($N_{s,out}$) (the sum is the total monomer number of the soot aggregates (N_s)). Here, the inner ($N_{s,in}$) and outer monomer numbers ($N_{s,out}$) are equal ($(1/2)N_s$) for the semi-embedded soot containing mixtures (Fig. 2).

The morphological parameters of different mixing states models are based on the results of in-situ and laboratory measurements. Bond and Bergstrom [7] reported the value of mean radius of monomer a in the range of 0.01–0.025 μm. In this study, the mean radius of the monomer $a = 0.015\ \mu m$ is assumed constant. The fractal dimension D_f of aged soot aerosols varies over a range of about 2.0–2.5 [43,23]. In this study, the fractal dimension $D_f = 2.2$ is assumed constant. To investigate the effects of atmospheric water on optical properties of soot aerosols, the assumptions of number of the monomers N_s is 60, and the fractal prefactor $k_0 = 1.2$. The volume-equivalent radius R of internally mixed aerosols lies typically in the range between 0.05 and 0.5 μm [23]. In this study, the radius of sulfate particle $R_{su} = 0.15\ \mu m$ is assumed constant. The volumes of sulfate and water remain same in every situation, meaning that the outer coatings (sulfate/water) would be larger for the semi-embedded and internal mixtures due to the volumetric effects of the inserts. The random orientation scattering properties are obtained analytically from the MSTM software, and these results are averaged by multiple calculations for 10 different clusters with the same morphological parameters.

The refractive indices of the pure black carbon particles are the values reported by Chang and Charalampopoulos [11], which lie in the range specified by Bond and Bergstrom [7]. The refractive indices of sulfate and atmospheric water are obtained from the OPAC database [18]. Table 1 shows the refractive indices of the soot aerosols.

3. The effect of atmospheric water on the optical properties of the soot aerosols

To quantify the effects of the atmospheric water on the optical properties of the soot aerosols in different mixing states, the MSTM version 3.0 (Multiple Sphere T-Matrix) was used to reconstruct the absorption and scattering

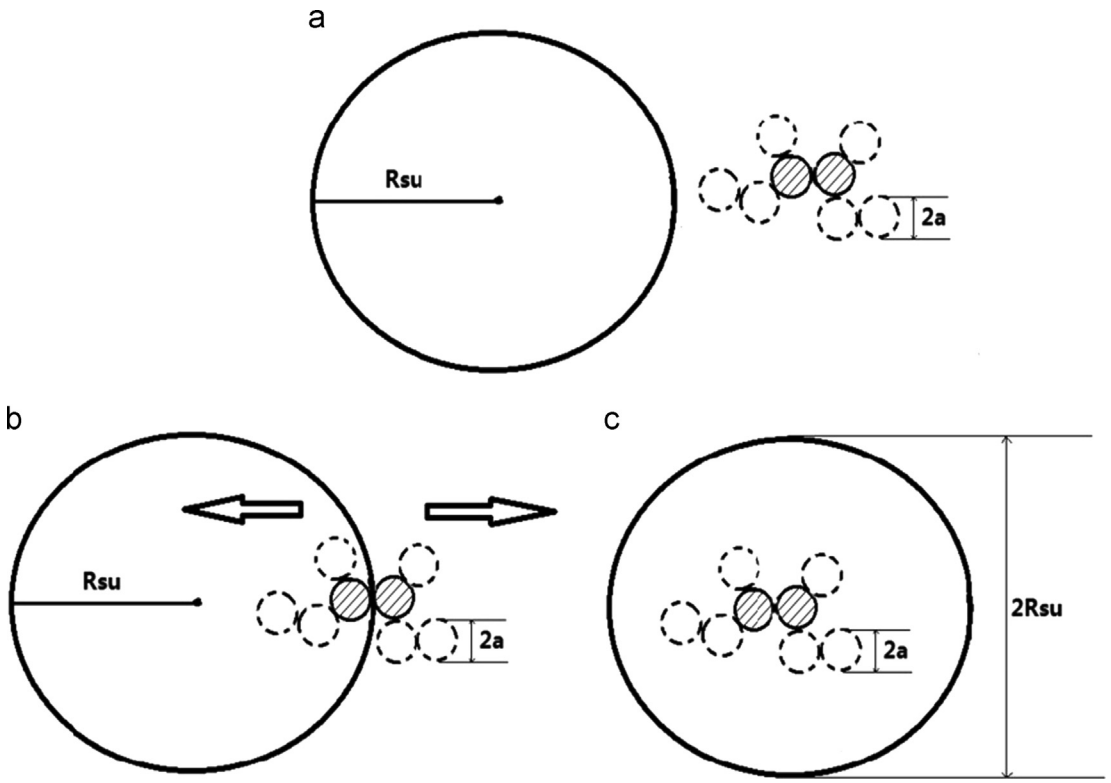

Fig. 2. Models of the three mixing states using the DLA method ((a) external mixtures, (b) semi-embedded mixtures, and (c) internal mixtures).

Table 1
The refractive indices of the different aerosol components.

Wavelength (μm)	Black carbon	Sulfate	Water
0.440	$m=1.70+0.64i$	$m=1.44$	$m=1.34$
0.670	$m=1.76+0.57i$	$m=1.44$	$m=1.33$
0.870	$m=1.79+0.57i$	$m=1.44$	$m=1.32$
1.020	$m=1.81+0.58i$	$m=1.44$	$m=1.32$

properties of the soot aerosols in three mixing states at different wavelengths (0.440 μm, 0.670 μm, 0.870 μm, and 1.020 μm), extending the formulation to arbitrary configurations of spherical surfaces. The spheres can be located internally or externally relative to each other while obeying the following constraint: a surface cannot intersect (or cut) any other surface. The version 3.0 software (codes, documentation, input files, and executables for serial windows machines) can be downloaded from http://www.eng.auburn.edu/users/dmckwski/scatcodes/.

Fig. 3 shows the variations in the optical properties of the soot aerosols with three mixing states. The absorption cross sections of external mixtures states were independent of thickness of water shell on the surface of soot aerosols. For external mixtures states condition, the hydrophobic properties of BC cannot be changed without the sulfate being coated. Because soot does not interact with atmospheric water, there is no impact of the amount of water. The BC particles are the major contributors to the absorption of soot particles. For the semi-embedded and internal mixtures states, the absorption cross-sections were enhanced because the water shell enlarged the effect of lens. Increasing the atmospheric water content increased the size of the water shell, reaching up to 40%.

Mixing the soot aerosols with atmospheric water changed the scattering properties dramatically (the single scattering albedo and the asymmetry parameter) even for the external mixture states (Figs. 4 and 5). The single scattering albedo of the soot aerosols was enhanced relative to that under dry conditions. The larger water shell induces stronger scattering. Decreasing the size parameter ($x=\pi D/\lambda$, where D is the particle diameter, λ is the wavelength) increased the scattering, reaching 54% at 1.020 μm. The asymmetry parameter exhibits a similar yet larger enhancement, reaching 3-fold at 1.020 μm. The asymmetry parameter increased when increasing the diameter of the water shell. A larger asymmetry parameter (stronger forward scattering) indicates that the incoming radiation is scattered back to its source less.

Provided that the radii of sulfate particle remain constant, the effect of atmospheric water on the optical properties of soot aerosols depends mostly on the mixing states of soot aerosols with sulfate and atmospheric water. Our studies show that the radiative absorption of the soot aerosols is enhanced due to the atmospheric water, which is accompanied by a large increase in scattering; the increased scattering is reflected by the increased single scattering albedo. The asymmetry parameter also increased when increasing the diameter of the water shell. Several studies [5,42] have shown that increasing the radiative

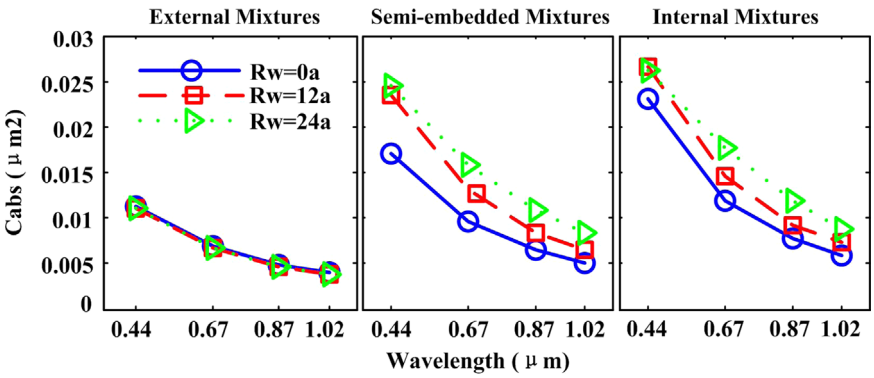

Fig. 3. Absorption coefficient of the soot aerosols with three mixing states (external, semi-embedded, internal). The different colors correspond to the optical properties of soot aerosols with different water contents (three representatives R_w: 0*a* (0 μ*m*), 12*a* (0.18 μ*m*), 24*a* (0.36 μ*m*)). (For interpretation of the references to color in this figure legend, the reader is referred to the web version of this article.)

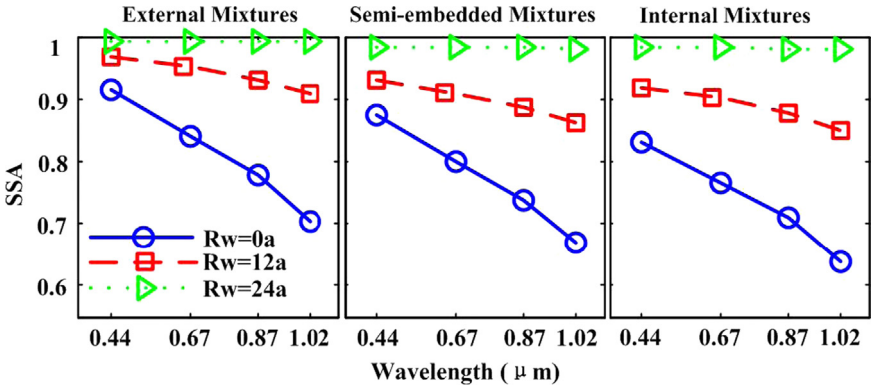

Fig. 4. Single scattering albedo of the soot aerosols with three mixing states (external, semi-embedded, internal). The different colors correspond to the optical properties of soot aerosols with different water contents (three representatives R_w: 0*a* (0 μ*m*), 12*a* (0.18 μ*m*), 24*a* (0.36 μ*m*)). (For interpretation of the references to color in this figure legend, the reader is referred to the web version of this article.)

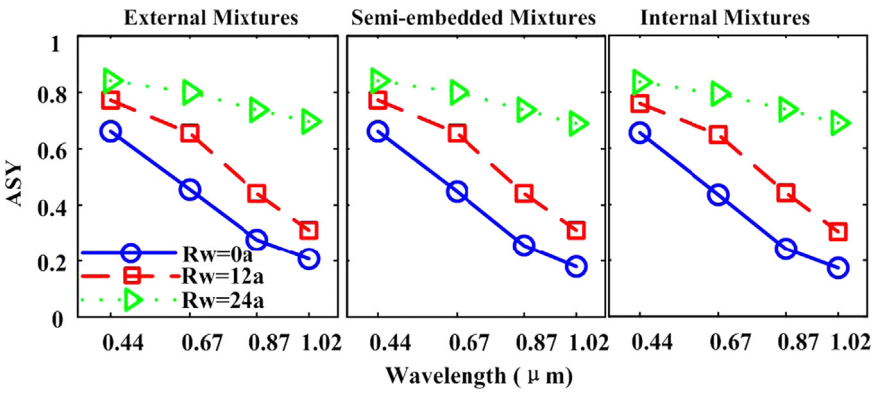

Fig. 5. Asymmetry parameters of the soot aerosols with three mixing states (external, semi-embedded, and internal). The different colors correspond to the optical properties of soot aerosols with different water contents (three representatives R_w: 0*a* (0 μ*m*), 12*a* (0.18 μ*m*), 24*a* (0.36 μ*m*)). (For interpretation of the references to color in this figure legend, the reader is referred to the web version of this article.)

absorption can exert a higher positive direct radiative force. In contrast, the enhanced single scattering albedo and asymmetry parameter can decrease the solar radiation absorption into the atmospheric layer [52,4]. Radiative forcing calculations suggest that a 10% decrease in the asymmetry parameter would cause a 19% reduction in the atmospheric radiative force [3,15].

4. The morphological effect of pure black carbon on the optical properties of the soot aerosols

Several studies show that the optical properties of the soot aerosols depend strongly on the morphology of the pure black carbon particles [32,54,12]. Yin and Liu [50] have investigated the effects of water coating on the

radiative properties of soot fractal aggregates in atmosphere, and found that the effect of change in morphology on the radiative properties cannot be neglected in wet air. They approximately look as aggregates composed of spherules attached to each other, which are individual primary spheres core coatings with water shell. They believe that soot fractal aggregates are hydrophilic, which can be coated by water directly.

The mixing states of BC particles with other aerosol particles and atmospheric water in this study are different with the mode assumed by Yin and Liu (2010). In this study, the pure BC is mixed with other water-soluble particles (sulfates). Coating of BC particles with water-soluble compound changes their hygroscopic properties, which tend to be hydrophilic. The coating (sulfates and atmospheric water) is much larger than the primary

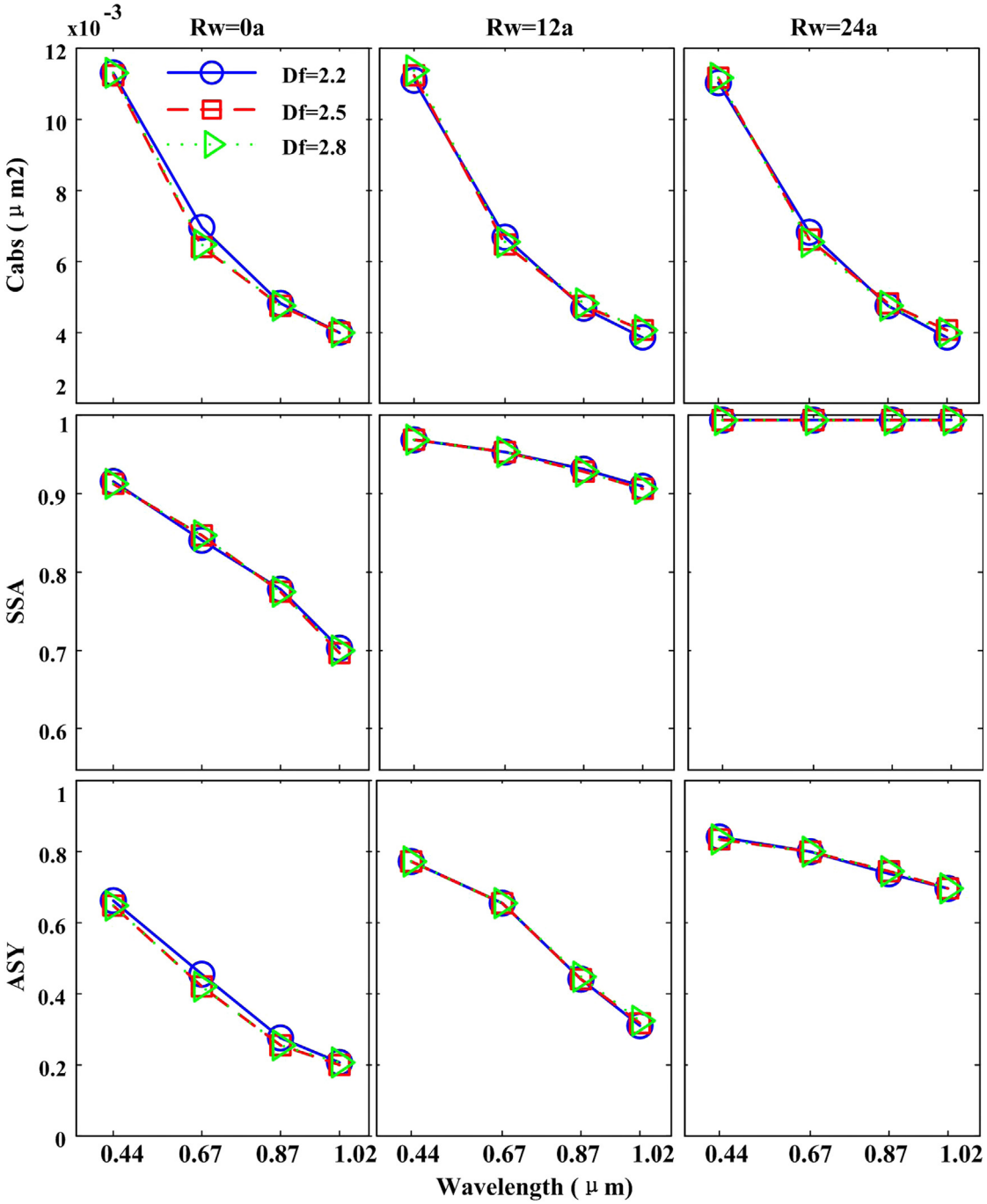

Fig. 6. Sensitivity of pure black carbon morphologies (three fractal dimensions are chosen to represent the compactness of particles: 2.2, 2.5, 2.8) toward the optical properties (cross sections of absorption, single scattering albedo (SSA) and asymmetry parameters (ASY)) of the soot aerosols with different atmospheric water contents in the external mixtures.

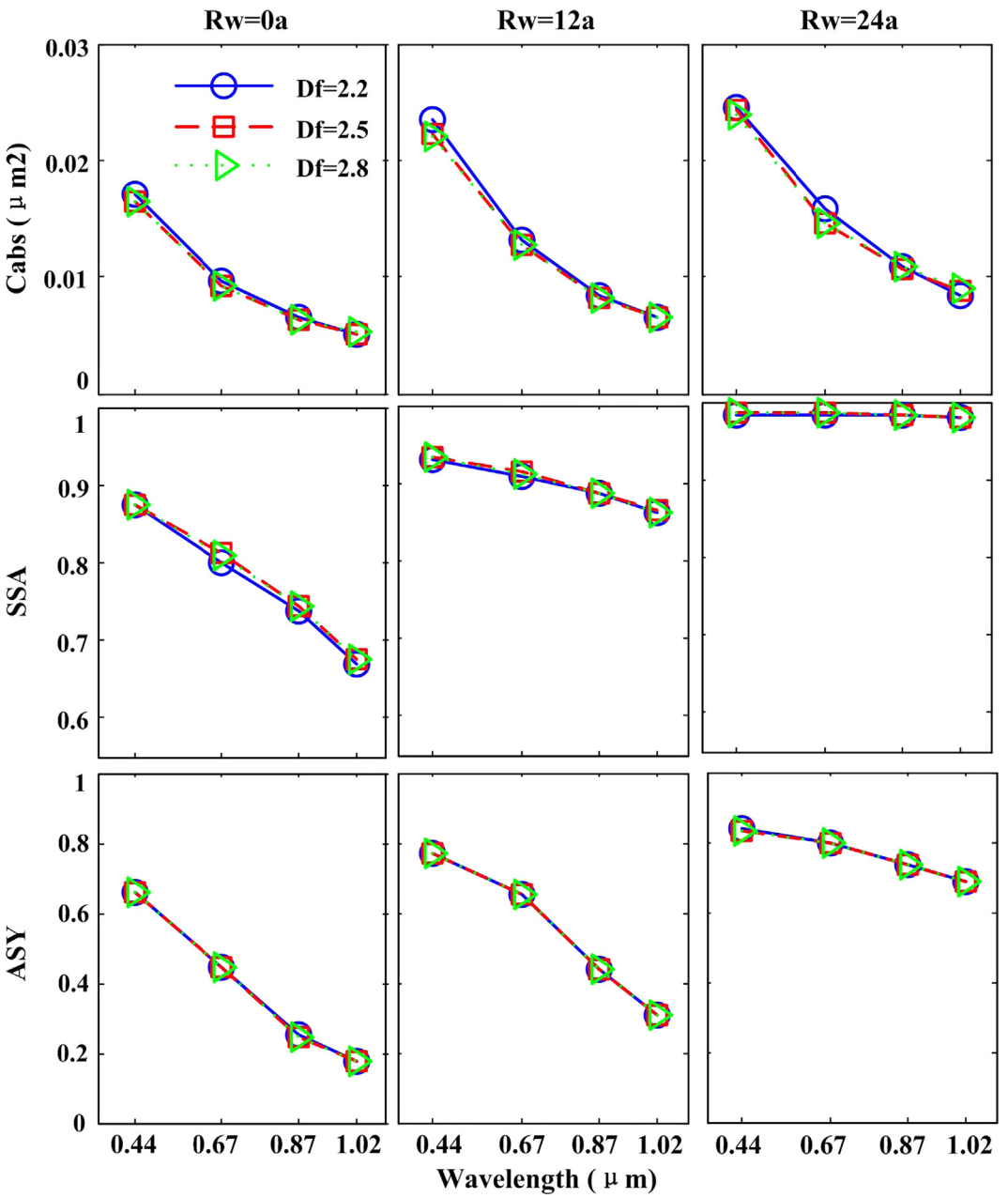

Fig. 7. Sensitivity of pure black carbon morphologies (three fractal dimension are chosen to represent the compactness of particles: 2.2, 2.5, 2.8) toward the optical properties (cross sections of absorption, single scattering albedo (SSA) and asymmetry parameters (ASY)) of the soot aerosols with different atmospheric water contents in the semi-embedded mixtures.

sphere of BC particles. The sensitivity of pure black carbon morphologies toward the optical properties of soot aerosols with three mixing states is investigated. Three fractal dimensions of BC particles represent the compactness of the particles: 2.2, 2.5, and 2.8.

Figs. 6–8 show that compared to previous studies, our results reveal only negligible morphological effects (fractal dimension) from pure black carbon on the optical properties of the soot aerosols with three mixing states. The morphological effects (fractal dimension) on the soot aerosols are weakened by contribution of sulfate and atmospheric water.

5. Enhancement in the optical properties due to the mixing state of the soot aerosols

Our theoretical simulation studies indicate that atmospheric water can affect the radiative absorption enhancement based on the mixing states of soot aerosols. In this study, the enhancement was defined as the ratio between the optical properties of the semi-embedded/internal mixing state and the optical properties of the external mixing state.

The absorption enhancements attributed to mixing state can reach 2-fold when pure BC is internally mixed

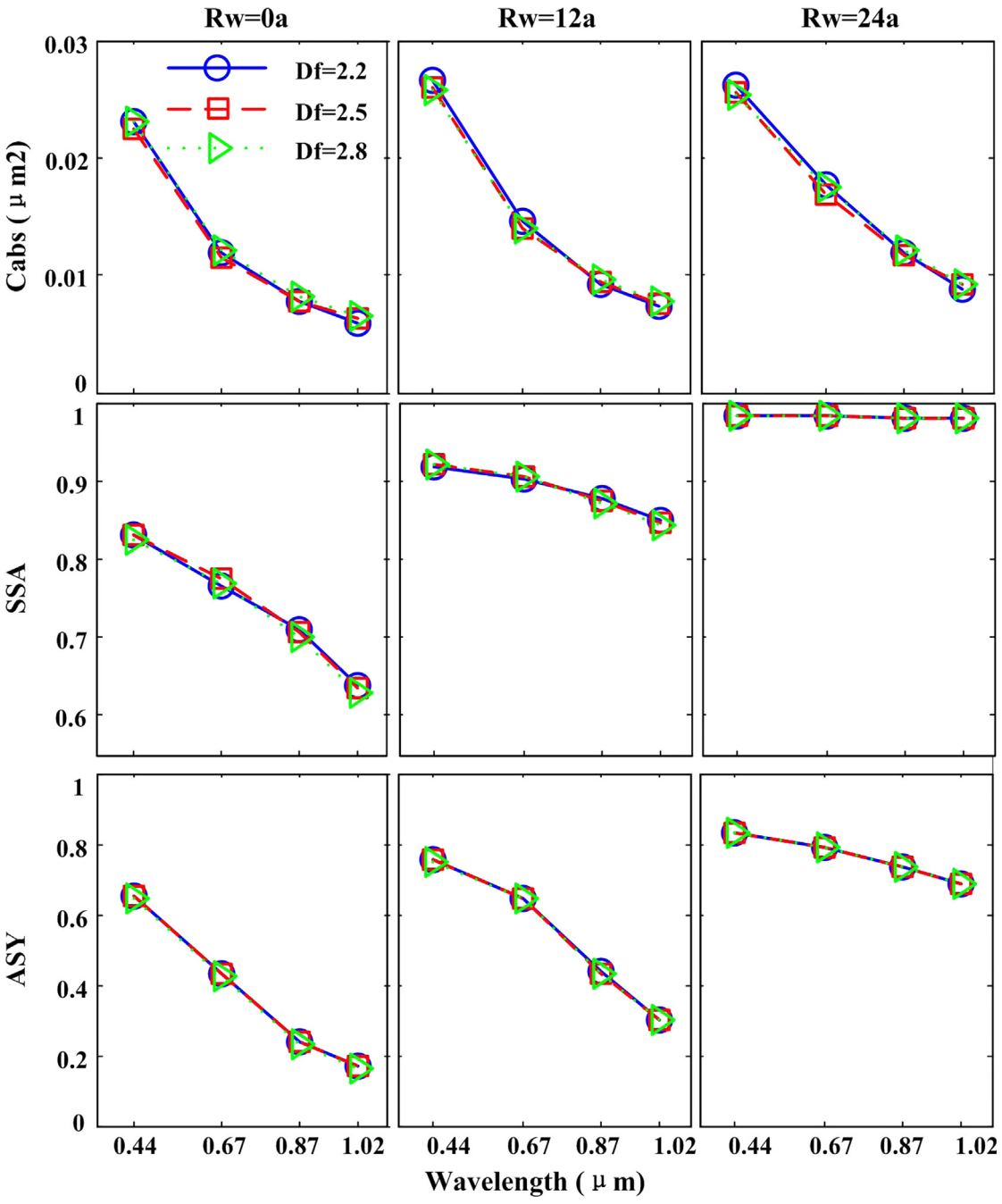

Fig. 8. Sensitivity of pure black carbon morphologies (three fractal dimension are chosen to represent the compactness of particles: 2.2, 2.5, 2.8) toward the optical properties (cross sections of absorption, single scattering albedo (SSA) and asymmetry parameters (ASY)) of the soot aerosols with different atmospheric water contents in the internal mixtures.

with sulfate particles without water compared to the external mixture. When the absorption is calculated, while accounting for the atmospheric water, the absorption enhancement increases, reaching a 2.5-fold increase. The difference in the absorption enhancements between the semi-embedded mixing state and the external mixing state is smaller, ranging from 1.5 (for no water) to 2.2 at 0.44 μm. The smaller absorption enhancements for semi-embedded mixing state occur due to the larger water shell effect obtained for the internal mixing state compared to the semi-embedded mixing state (Figs. 9 and 10).

In addition, the effects of the atmospheric water on the scattering ability attributed to the mixing states have also been investigated. In contrast, the scattering ability decreased when the BC is in semi-embedded/internal mixing states instead of the external mixing state. When the R_w is 0a (for no water), the SSA reduction can reach 10% for internal mixing state, while the SSA reduction for

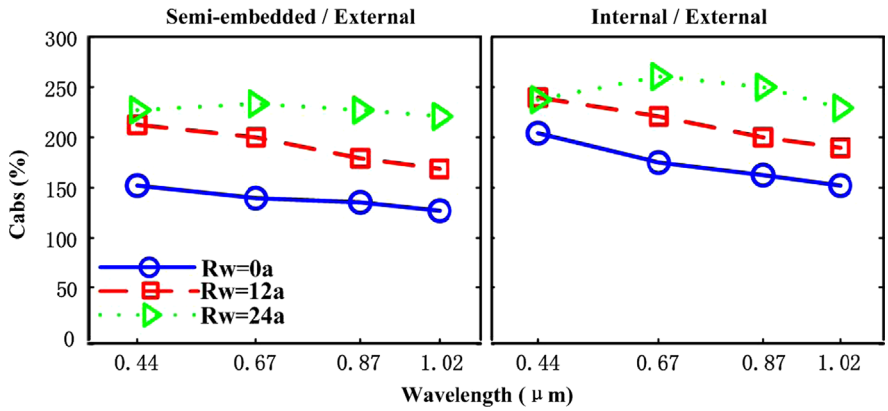

Fig. 9. Ranges for the absorption enhancement attributed to the mixing states of the soot aerosols. The absorption enhancement is increased after accounting for the atmospheric water effects. The wavelengths used for the calculations were 0.440, 0.670, 0.870, and 1.020 μm.

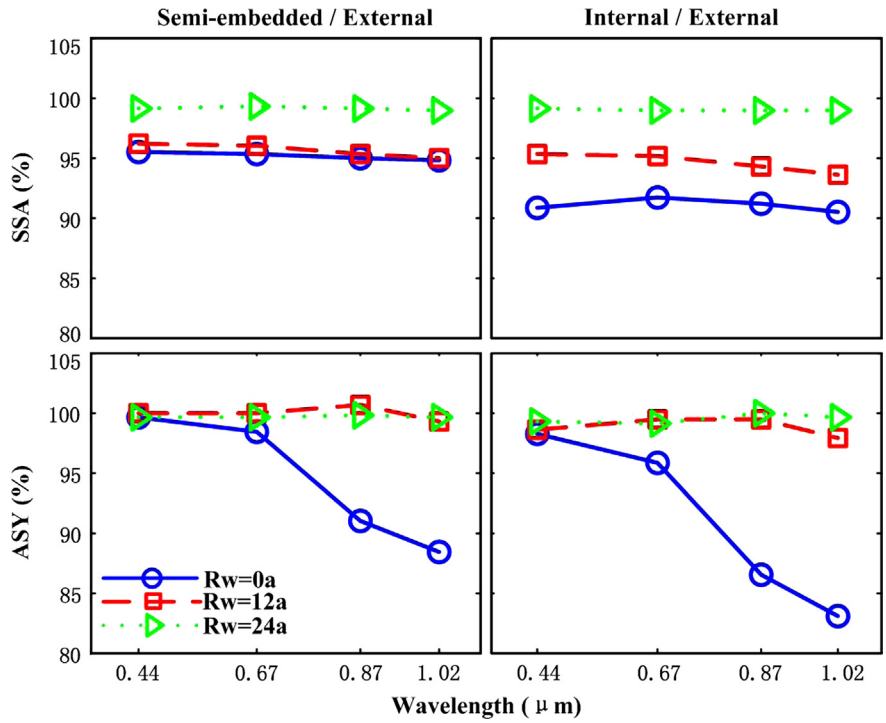

Fig. 10. Ranges for the reduction in scattering due to the mixing states of soot aerosols. The wavelengths used for the calculations were 0.440, 0.670, 0.870, and 1.020 μm.

the semi-embedded mixing state is smaller, reaching 5%. After accounting for the effect of the atmospheric water, the SSA reduction decreased (less than 1%). The effect of the mixing states on the ASY is small, especially with water, and this can be ignored.

6. Conclusions and discussion

The effects of the atmospheric water on the optical properties of the soot aerosols were studied theoretically while accounting for the mixing mechanism utilized by the black carbon with other aerosol particles and atmospheric water at different wavelengths (0.440, 0.670, 0.870, and 1.020 μm).

Based on the transmission electron microscopy measurements and the hygroscopic properties of the soot aerosols, three mixing states with and without water were modeled: externally mixed; semi-embedded mixed and internally mixed. MSTM version 3.0 (Multiple Sphere T-Matrix) was used to reconstruct the absorbance and scattering properties of the soot aerosols in the three mixing states.

An increased absorption is accompanied by an enhanced scattering ability attributed to the atmospheric water on the surfaces of the soot aerosols, which has an opposing effect on climate change. The absorption of the external mixtures states remained independent of the atmospheric water, while the semi-embedded mixtures states and internal mixtures

states showed enhanced absorption cross sections because the water shell increases the lens effect. Increasing atmospheric water content resulted in growth of water shell, and the enhancement can reach 40%. Mixing the soot particles with water changed the scattering properties of soot aerosols dramatically, even for the external mixtures. The single scattering albedo of the soot aerosols was enhanced relative to that under dry conditions. Decreasing the size parameter increased the scattering enhancement, reaching 54%. The asymmetry parameter has a similar yet larger enhancement, reaching three-fold.

Compared to previous studies, our results reveal only negligible morphological effects (fractal dimension) from pure black carbon on the optical properties of the soot aerosols with three mixing states. The morphological effects on the soot aerosols are weakened by contribution of sulfate and atmospheric water.

In addition, the atmospheric water increased the enhancement of the radiative absorption based on the mixing states of the soot aerosols from 1.5- to 2.5-fold on average at 0.870 μm. The semi-embedded/internal mixing states have a smaller single scattering albedo and asymmetry parameter than the externally mixing states. When the water content increased, the differences in the scattering ability of the soot aerosols in the three mixing states decreased.

The high sensitivity of the optical properties of the soot toward the atmospheric water content reveals that the effect of soot aerosols exerted on climate change cannot be evaluated accurately until the effects of the atmospheric water on the optical properties of the soot aerosol in different mixing states are known.

Acknowledgments

We would like to acknowledge the authors of the superposition T-matrix: Daniel Mackowski, Kirk Fuller, and Michael Mishchenko. The code for the superposition T-matrix was downloaded from http://www.eng.auburn.edu. This research was supported by the National Basic Research Program of China (973 Program) (Grant no. 2010CB950800), the National Natural Science Foundation of China (Grant no. 41371015, 41001207) and the Strategic Priority Research Program of the Chinese Academy of Sciences, Climate Change: Carbon Budget and Relevant Issues (Grant no. XDA05100203). The data used to produce the results of this paper were simulated using the code of superposition T-matrix.

References

[1] Adachi K, Chung SH, Buseck PR. Shapes of soot aerosol particles and implications for their effects on climate. J Geophys Res 2010;115:D15206. http://dx.doi.org/10.1029/2009JD012868.
[2] Adachi K, Chung SH, Friedrich H, Buseck PR. Fractal parameters of individual soot particles determined using electron tomography: implications for optical properties. J Geophys Res 2007;112:D14202. http://dx.doi.org/10.1029/2006JD008296.
[3] Andrews E, Sheridan PJ, Fiebig M, McComiskey A, Ogren JA, Arnott P, et al. Comparison of methods for deriving aerosol asymmetry parameter. J Geophys Res 2006;111:D05S04, http://dx.doi.org/10.1029/2004JD005734.
[4] Bergstrom RW, Russell PB, Hignett P. Wavelength dependence of the absorption of black carbon particles: predictions and results from the TARFOX experiment and implications for the aerosol single scattering albedo. J Atmos Sci 2002;59:567–77.
[5] Bond TC, Doherty SJ, Fahey DW, Forster PM, Berntsen T, DeAngelo BJ, et al. Bounding the role of black carbon in the climate system: a scientific assessment. J Geophys Res 2013;118:5380–552.
[6] Bond TC, Habib G, Bergstrom RW. Limitations in the enhancement of visible light absorption due to mixing state. J. Geophys. Res. 2006;111(D20):211. http://dx.doi.org/10.1029/2006JD007315.
[7] Bond TC, Bergstrom RW. Light absorption by carbonaceous particles: an investigative review. Aerosol Sci Technol 2006;40(1):27–67.
[8] Cappa CD, Onasch TB, Massoli P, Worsnop DR, Bates TS, Cross ES, et al. Radiative absorption enhancements due to the mixing state of atmospheric black carbon. Science 2012;337:1078–81, http://dx.doi.org/10.1126/science.1223447.
[9] Cappa CD, Onasch TB, Massoli P, Worsnop DR, Bates TS, Cross ES, Davidovits Paul, Hakala Jani, et al. Response to Comment on "Radiative absorption enhancements due to the mixing state of atmospheric black carbon". Science 2013;339:393.
[10] Carrico CM, Petters MD, Kreidenweis SM, Sullivan AP, McMeeking GR, Levin EJT, et al. Water uptake and chemical composition of fresh aerosols generated in open burning of biomass. Atmos Chem Phys 2010;10:5165–78. http://dx.doi.org/10.5194/acp-10-5165-2010.
[11] Chang H, Charalampopoulos TT. Determination of the wavelength dependence of refractive indices of flame soot. Proc R Soc Lond A 1990;430:577–91.
[12] Cheng T, Gu X, Wu Y, Chen H, Yu T. The optical properties of absorbing aerosols with fractal soot aggregates: implications for aerosol remote sensing. J Quant Spectrosc Radiat Transf 2013;125:93–104.
[13] China S, Mazzoleni C, Gorkowski K, Aiken AC, Dubey MK. Morphology and mixing state of individual freshly emitted wildfire carbonaceous particles. Nat Commun 2013;4:2122. http://dx.doi.org/10.1038/ncomms3122.
[14] Chung SH, Seinfeld JH. Climate response of direct radiative forcing of anthropogenic black carbon. J Geophys Res 2005;110(D11):102. http://dx.doi.org/10.1029/2004JD005441.
[15] Fiebig M, Ogren JA. Retrieval and climatology of the aerosol asymmetry parameter in the NOAA aerosol monitoring network. J Geophys Res 2006;111:D21204. http://dx.doi.org/10.1029/2005JD006545.
[16] Hand JL, Day DE, McMeeking GM, Levin EJT, Carrico CM, Kreidenweis SM, et al. Measured and modeled humidification factors of fresh smoke particles from biomass burning: role of inorganic constituents. Atmos Chem Phys 2010;10:6179–94. http://dx.doi.org/10.5194/acp-10-6179-2010.
[17] Haywood JM, Ramaswamy V. Global sensitivity studies of the direct radiative forcing due to anthropogenic sulfate and black carbon aerosols. J Geophys Res 1998;103(D6):6043–58.
[18] Hess M, Koepke P, Schult I. Optical properties of aerosols and clouds: the software package OPAC. Bull Am Meteorol Soc 1998;79:831–44.
[19] Intergovernment Panel on Climate Change. Climate change 2007: the physical science basis-working group I Contribution to the IPCC 4th assessment report of the Intergovernmental Panel on Climate Change. In: Solomon S, et al., editors. Cambridge UK and New York, USA: Cambridge University Press; 2007.
[20] Ishiguro T, Takatori Y, Akihama K. Microstructure of diesel soot particles probed by electron microscopy: first observation of inner core and outer shell. Combust Flame 1997;108(10):231–4.
[21] Jacobson MZ. Strong radiative heating due to the mixing state of black carbon in atmospheric aerosols. Nature 2001;409:695–7.
[22] Jacobson MZ. Comment on "Radiative absorption enhancements due to the mixing state of atmospheric black carbon". Science 2013;339:393.
[23] Kahnert M, Nousiainen T, Lindqvist H. Models for integrated and differential scattering optical properties of encapsulated light absorbing carbon aggregates. Opt Exp 2013;21(7):7974–93.
[24] Kahnert M. Modelling the optical and radiative properties of freshly emitted light absorbing carbon within an atmospheric chemical transport model. Atmos Chem Phys 2010;10:1403–16.
[25] Kahnert M, Nousiainen T, Räisänen P. Mie simulations as an error source in mineral aerosol radiative forcing calculations. Q J R Meteorol Soc 2007;133:299–307.
[26] Kahnert M, Nousiainen T, Veihelmann B. Spherical and spheroidal model particles as an error source in aerosol climate forcing and radiance computations: a case study for feldspar aerosols. J Geophys Res 2005;110:D18S13. http://dx.doi.org/10.1029/2004JD005558.

[27] Khalizov AF, Xue HX, Wang L, Zheng J, Zhang R. Enhanced light absorption and scattering by carbon soot aerosol internally mixed with sulfuric acid. J Phys Chem A 2009;113:1066–74.
[28] Khalizov AF, Zhang R, Zhang D, Xue H, Pagels J, McMurry PH. Formation of highly hygroscopic soot aerosols upon internal mixing with sulfuric acid vapor. J Geophys Res 2009;114:D05208. http://dx.doi.org/10.1029/2008JD010595.
[29] Kis VK, Pósfai M, Lábár JL. Nanostructure of atmospheric soot particles. Atmos Environ 2006;40(29):5533–42.
[30] Lack DA, Langridge JM, Bahreini R, Cappa CD, Middlebrook AM, Schwarz JP. Brown carbon and internal mixing in biomass burning particles. Proc Natl Acad Sci USA 2012;109(37):14802–7.
[31] Li J, Pósfai M, Hobbs PV, Buseck PR. Individual aerosol particles from biomass burning in southern Africa: 2, Compositions and aging of inorganic particles. J Geophys Res 2003;108(D13):8484, http://dx.doi.org/10.1029/2002JD002310.
[32] Liu L, Mishchenko MI. Effects of aggregation on scattering and radiative properties of soot aerosols. J Geophys Res 2005;110:D11211.
[33] Liu L, Mishchenko MI. Scattering and radiative properties of complex soot and soot-containing aggregate particles. J Quant Spectrosc Radiat Transf 2007;106:262–73.
[34] Logan BE, Kilps JR. Fractal dimensions of aggregates formed in different fluid mechanical environments. Water Res 1995;29:443–53.
[35] Mackowski DW. A general superposition solution for electromagnetic scattering by multiple scattering domains of optically active media. J Quant Spectrosc Radiat Transf 2014;133:264–70.
[36] Mackowski DW, Mishchenko MI. Calculation of the T matrix and the scattering matrix for ensembles of spheres. J Opt Soc Am A 1996;13:2266–78.
[37] Matsui H, Koike M, Kondo Y, Moteki N, Fast JD, Zaveri RA. Development and validation of a black carbon mixing state resolved three-dimensional model: aging processes and radiative impact. J Geophys Res 2013;118:5.
[38] Mishchenko MI, Li L, Mackowski DW. T-matrix modeling of linear depolarization by morphologically complex soot and soot-containing aerosols. J Quant Spectrosc Radiat Transf 2013;123:135–44.
[39] Mishchenko MI. Electromagnetic scattering by nonspherical particles: a tutorial review. J Quant Spectrosc Radiat Transf 2009;110:808–32.
[40] Mikhailov EF, Vlasenko SS, Podgorny IA, Ramanathan V, Corrigan CE. Optical properties of soot–water drop agglomerates: an experimental study. J Geophys Res 2006;111:D07209. http://dx.doi.org/10.1029/2005JD006389.
[41] Mikhailov EF, Vlasenko SS, Krämer L, Niessner R. Interaction of soot aerosol particles with water droplets: influence of surface hydrophilicity. J Aerosol Sci 2001;32:697–711.
[42] Myhre G. Consistency between satellite-derived and modeled estimates of the direct aerosol effect. Science 2009;325:187–90.
[43] Nyeki S, Colbeck I. Fractal dimension analysis of single, in-situ, restructured carbonaceous aggregates. Aerosol Sci Technol 1995;23(2):109–20.
[44] Popovicheva O, Persiantseva NM, Shonija NK, DeMott P, Koehler K, Petters M, et al. Water interaction with hydrophobic and hydrophilic soot particles. Phys Chem Chem Phys 2008;10:2332–44.
[45] Popovicheva O, Persiantseva NM, Tishkova V, Shonija NK, Zubareva NA. Quantification of water uptake by soot particles. Environ Res Lett 2008;3:025009. http://dx.doi.org/10.1088/1748-9326/3/2/025009.
[46] Pósfai M, Simonics R, Li J, Hobbs PV, Buseck PR. Individual aerosol particles from biomass burning in southern Africa: 1. Compositions and size distributions of carbonaceous particles. J Geophys Res 2003;108(D13):8483. http://dx.doi.org/10.1029/2002JD002291.
[47] Ramanathan V, Carmichael G. Global and regional climate changes due to black carbon. Nat Geosci 2008;1(4):221–7.
[48] Schnaiter M, Linke C, Möhler O, Naumann K-H, Saathoff H, Wagner R, et al. Absorption amplification of black carbon internally mixed with secondary organic aerosol. J Geophys Res 2005;110(D19):204. http://dx.doi.org/10.1029/2005JD006046.
[49] Schwarz JP, Gao RS, Spackman JR, Watts LA, Thomson DS, Fahey DW, et al. Measurement of the mixing state, mass, and optical size of individual black carbon particles in urban and biomass burning emissions. Geophys Res Lett 2008;35(13):810. http://dx.doi.org/10.1029/2008GL033968.
[50] Yin JY, Liu LH. Influence of complex component and particle polydispersity on radiative properties of soot aggregate in atmosphere. J Quant Spectrosc Radiat Transf 2010;111:2115–26.
[51] Slowik JG, Cross ES, Han J-H, Davidovits P, Onasch TB, Jayne JT, et al. An inter-comparison of instruments measuring black carbon content of soot particles. Aerosol Sci Technol 2007;41(3):295–314.
[52] Takemura T, Nakajima T, Dubovik O, Holben BN, Kinne S. Single-scattering albedo and radiative forcing of various aerosol species with a global three-dimensional model. J Clim 2002;15:333–52.
[53] Weingartner E, Burtscher H, Baltensperger U. Hygroscopic properties of carbon and diesel soot particles. Atmos Environ 1997;31(15):2311–27.
[54] Wu Y, Gu X, Cheng T, Xie D, Yu T, Chen H, et al. The single scattering properties of the aerosol particles as aggregated spheres. J Quant Spectrosc Radiat Transf 2012;113:1454–66.
[55] Zhang R, Khalizov AF, Pagels J, Zhang D, Xue H, McMurry PH. Variability in morphology, hygroscopicity, and optical properties of soot aerosols during atmospheric processing. Proc Natl Acad Sci USA 2008;105(30):10291–6.
[56] Zuberi B, Johnson KS, Aleks GK, Molina LT, Molina MJ, Laskin A. Hydrophilic properties of aged soot. Geophys Res Lett 2005;32:L01807. http://dx.doi.org/10.1029/2004GL021496.